The Journal of Green Energy and Environmental Engineering

Research Paper

Preparation and Properties of Dual-Network Upper Critical Solution Temperature-Type Deep Profile Control Slow-Swelling Particles

Kristen M. Logue[1,*], Mary Favela[1], Calorin Lennard[2]

[1] National Centre for Forensic Studies (NCFS), Faculty of Science and Technology, University of Canberra, Canberra, Australia
[2] UCL University College, Kolding, Denmark
*Corresponding author: KLogue@canberra.edu.au; MFa@hotmail.com; cale.geog@hotmail.com

Abstract. A dual-network upper critical solution temperature (UCST)-type hydrogel, poly(methyl methacrylamide)/poly(N,N-dimethylacrylamide) (PMAAm/PDMAA), was prepared via free radical polymerization and a soaking method using methyl methacrylamide (MAAm) and N,N-dimethylacrylamide (DMAA) as monomers, N,N-methylene bisacrylamide (BIS) as a crosslinking agent, and 2,2-diethoxyacetophenone (I-2959) as an initiator, for application in profile control and water plugging. The morphology, hydrogen bonding interactions, and temperature-responsive properties of the hydrogel were characterized by scanning electron microscopy (SEM), Fourier-transform infrared spectroscopy (FTIR), and a high-temperature rheometer. The swelling behavior in response to temperature and the influence of the ratio of hydrogen bond donors (amine groups) to hydrogen bond acceptors (carbonyl groups) on the mechanical properties of the hydrogel were investigated. The results showed that when the molar ratio of MAAm to DMAA was 2:1, the prepared dual-network UCST-type hydrogel (PMAAm/PDMAA-2.0) exhibited a high transition temperature (90 °C), a tensile strength of up to 13.8 MPa, a tensile strain at break of 100.9%, and a compressive strength of 4.0 MPa at 80% compressive strain. The UCST response of PMAAm/PDMAA-2.0 was primarily attributed to the association and dissociation of hydrogen bonds between polymer chains, which led to swelling resistance at low temperatures and significant water absorption and expansion (up to 40 times its original size) at high temperatures, with a breakthrough pressure of 0.65 MPa.

Keywords: *upper critical solution temperature; deep profile control; slow-swelling particles; hydrogen bonding entanglement; double network gels; oil field chemicals*

Received on 15 Feb 2026, Accepted on 15 May 2026, Published on 22 July 2026

1 Introduction

With the rapid development of China's economy and society, energy demand continues to rise, and the external dependency rate of energy remains persistently high, posing a serious threat to national energy security [1–3]. Mature oilfields in China account for a large proportion of reserves and production and remain the "ballast stone" for reserves, output, and economic benefits; however, their average recovery rate is only approximately 30%. Therefore, research on enhancing the recovery rate of mature oilfields is of great significance [4,5].

Due to long-term water injection for oil recovery in mature oilfields, the water cut in reservoirs has gradually increased, and high-permeability dominant channels have formed between injection wells and production wells, resulting in a large portion of low-permeability reservoirs remaining underdeveloped [6]. Currently, commonly used profile control agents, such as strong and weak gels formed by polyacrylamide-based polymers [7–10], are mainly effective in near-wellbore zones because they are easily diluted by formation water and have low mechanical strength, making it difficult to exert lasting effects in deep formations. To further improve deep profile control performance, researchers have developed bulk-swelling particles [11,12] and polymer gel microspheres [13–16] through pre-crosslinked polymers. Although these materials possess certain deep profile

control capabilities, their hydration and expansion rates are positively correlated with temperature, preventing effective suppression of expansion in low-temperature environments, and thus failing to meet the requirements of deep profile control at the current stage. In view of this, there is an urgent need to develop novel profile control agents capable of penetrating deep into formations effectively. Formation temperature, as a natural factor, provides a potential regulatory means. Temperature-sensitive gels, especially upper critical solution temperature (UCST)-type gels, have garnered widespread attention in recent years due to their ability to adjust hydrophilicity based on temperature changes. UCST-type gels can transition to a hydrophilic state and absorb water to swell at specific high temperatures, while remaining in a hydrophobic state at low temperatures. This characteristic gives UCST-type gels a distinct advantage in deep profile control and plugging applications, as they can effectively respond to changes in formation temperature, thereby optimizing the profile control effect in oil and gas recovery.

LI et al. [17] prepared gel particles exhibiting UCST properties by crosslinking and modifying polyethylene glycol with glutaraldehyde; these particles demonstrated strong expansion capability at high temperatures while remaining suppressed at low temperatures. LE et al. [18] prepared double thermosensitive nanogel particles using poly(methyl methacrylate) and poly(2-hydroxyethyl methacrylate) with different UCST transition temperatures, which achieved multi-stage swelling at specific temperatures. However, the transition temperatures of most existing UCST-type gels are <60 °C, making it difficult to meet the demands of formation temperatures.

This study intends to construct a double-layer network structure gel based on strong hydrogen bonding interactions between polymer chains [19,20]. Poly(methyl methacrylamide)/poly(N,N-dimethylacrylamide) (PMAAm/PDMAA) dual-network UCST-type profile control agents were prepared sequentially via free radical polymerization and a soaking method, using methyl methacrylamide (MAAm) and N,N-dimethylacrylamide (DMAA) as monomers. The swelling properties under temperature response and the influence of the ratio of hydrogen bond donors (amine groups) to hydrogen bond acceptors (carbonyl groups) on the mechanical properties of the hydrogel were investigated. This study aims to provide technical references for the preparation of efficient and controllable deep profile control materials.

2 Experimental Section

2.1 Reagents and Instruments

MAAm, DMAA, N,N-methylene bisacrylamide (BIS), and 2,2-diethoxyacetophenone (I-2959) were of analytical grade and purchased from Chengdu Kelong Chemical Reagent Co., Ltd.

EVO MA15 scanning electron microscope (SEM), Carl Zeiss, Germany; HAAKE MARS II high-temperature rheometer and Nicolet 6700 Fourier-transform infrared spectrometer (FTIR), Thermo Fisher Scientific, USA; VERTEX 80v all-vacuum Fourier-transform infrared spectrometer (In-situ FTIR), Bruker, Germany; AG-X PLUS 50 kN universal testing machine, Shimadzu, Japan.

2.2 Sample Preparation

2.2.1 Preparation of PMAAm Gel

0.85 g (0.01 mol) of MAAm was dissolved in 2 mL of deionized water. Under stirring at 40 °C, 0.4% (by mass of MAAm, the same below) of crosslinking agent BIS and 1% of photoinitiator I-2959 were added. The mixture was stirred at 40 °C for 60 min to obtain the PMAAm hydrogel precursor solution. The solution was poured into a 20 mm × 20 mm × 5 mm mold and exposed to 365 nm ultraviolet light at a distance of 20 cm for 2 h to obtain the PMAAm gel.

2.2.2 Preparation of PDMAA Gel

0.50 g (0.005 mol) of DMAA, 0.4% (by mass of DMAA, the same below) of crosslinking agent BIS, and 1% of photoinitiator I-2959 were added to 2 mL of deionized water. After stirring at 40 °C for 60 min, the PDMAA gel

precursor solution was obtained. The solution was poured into a 30 mm × 20 mm × 5 mm mold and exposed to 365 nm ultraviolet light at a distance of 20 cm for 2 h to obtain the PDMAA gel.

2.2.3 Preparation of Dual-Network UCST-Type Profile Control Agent

2.00 g (0.02 mol) of DMAA, 0.4% (by mass of DMAA, the same below) of crosslinking agent BIS, and 1% of photoinitiator I-2959 were added to 8 mL of deionized water. After stirring at 40 °C for 60 min, the PDMAA gel precursor solution was obtained and set aside.

The PMAAm gel prepared in Section 1.2.1 was placed in a petri dish containing the reserved PDMAA gel precursor solution and soaked at 30 °C for 48 h. Then, the mixture was exposed to 365 nm ultraviolet light at a distance of 20 cm for 2 h to obtain a bulk dual-network UCST-type profile control agent (PMAAm/PDMAA). By changing the amount of MAAm in Section 1.2.1 and following the above preparation process, a series of PMAAm/PDMAA samples were obtained. PMAAm/PDMAA prepared with PMAAm to PDMAA concentration ratios of 1.0, 1.5, 2.0, and 2.5 were designated as PMAAm/PDMAA-1.0, PMAAm/PDMAA-1.5, PMAAm/PDMAA-2.0, and PMAAm/PDMAA-2.5, respectively.

Figure 1 shows a schematic diagram of the preparation process of PMAAm/PDMAA. The specific formulation is listed in Table 1.

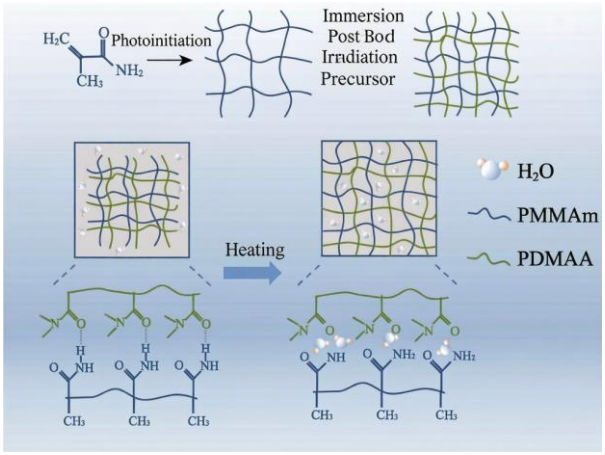

Figure 1 Schematic diagram of preparation process of PMAAm/PDMAA

Table 1 Formula of PMAAm/PDMAA

Sample name	MAAm/mol	V1/mL	DMAA/mol	V2/mL
PMAAm/PDMAA-1.0	0.0050	2	0.02	8
PMAAm/PDMAA-1.5	0.0075	2	0.02	8
PMAAm/PDMAA-2.0	0.0100	2	0.02	8
PMAAm/PDMAA-2.5	0.0125	2	0.02	8

2.3 Characterization Methods and Performance Testing

Before SEM, FTIR, and In-situ FTIR testing, gel samples were cryo-fractured in liquid nitrogen and freeze-dried for 72 h.

SEM testing: Samples were sputter-coated with gold and imaged in low-vacuum secondary electron (LEI) mode with a working current of 20 μA and an electron acceleration voltage of 20.0 kV.

FTIR testing: KBr pellet method, wavenumber range 4000–500 cm^{-1}, resolution 4 cm^{-1}, 32 scans.

In-situ FTIR testing: Samples were ground into a powder state. Temperature was increased from 30 to 150 °C at a heating rate of 5 °C/min, with a 10-min hold every 30 °C to characterize hydrogen bond association. Spectra were collected in single-beam mode with a resolution of 4 cm^{-1}, wavenumber range 4000–1200 cm^{-1}, using a liquid nitrogen-cooled MCT-B detector.

Rheological performance testing: The post-initiated PMAAm/PDMAA-2.0 was fixed on the rheometer testing platform. Temperature sweeps were performed at 1% strain from 40 to 100 °C, and frequency sweeps were performed from 100 to 0.1 Hz. The loss modulus (G'') and storage modulus (G') as functions of temperature and frequency were measured.

Swelling performance testing: 1 g (m0, g) of the post-initiated gel sample was completely immersed in 10 mL of deionized water and sealed. Swelling was conducted under heating conditions at different temperatures. The gel mass (mt, g) at different times (t, min) and the mass at swelling equilibrium (mmax, g) at different temperatures were recorded. Surface water was removed before weighing, and each group was tested in triplicate to obtain arithmetic mean values. The swelling ratio (R, %) and equilibrium swelling ratio (Re, %) were calculated according to Equations (1) and (2):

$$R/\% = (mt - m0)/m0 \times 100 \quad (1)$$

$$Re/\% = (mmax - m0)/m0 \times 100 \quad (2)$$

Uniaxial tensile test: Post-initiated gels were cut into rectangular prisms measuring 60 mm × 5 mm × 2 mm. During stretching, the load was maintained at 200 N with a stretching rate of 10 mm/min until the gel fractured. Each sample was tested at least three times, and the arithmetic mean was taken as the result.

Compression test: Post-initiated gels were shaped into cylinders (Φ 10 mm × 20 mm). The compression rate was maintained at 2 mm/min until the gel ruptured or the strain reached 80%, at which point compression stopped. Each sample was tested at least three times, and the arithmetic mean was taken as the result.

2.4 Plugging Simulation Experiment

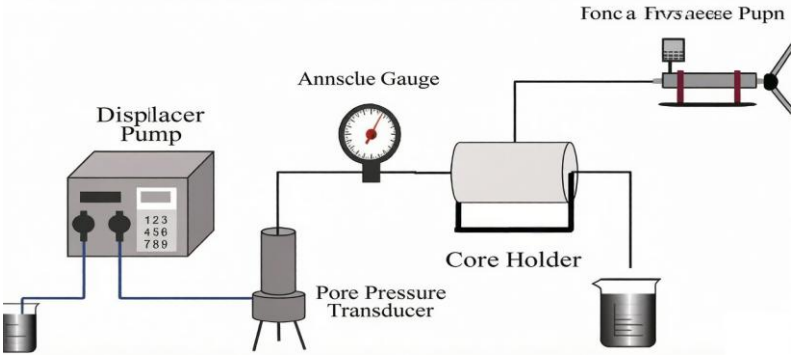

Figure 2 Schematic diagram of plugging simulator

A stainless-steel core with dimensions Φ 25.4 mm × 50 mm, fracture aperture of 2.0 mm, and fracture width of 10 mm was used to simulate formation temperature conditions. Gel particles smaller than 1 mm were dried at 70 °C for 24 h and placed into the core fracture. After the gel particles reached swelling equilibrium within the fracture, the experiment was conducted at a flow rate of 0.5 mL/min. Pressure gauge data changes were recorded, and the experiment ended once the pressure stabilized, determining the breakthrough pressure of the profile control agent. Figure 2 shows a schematic diagram of the experimental setup.

3 Results and Discussion

3.1 Characterization of Samples

3.1.1 FTIR Analysis

Figure 3 shows the FTIR spectra of freeze-dried PMAAm/PDMAA-2.0, PDMAA gel, and PMAAm gel samples.

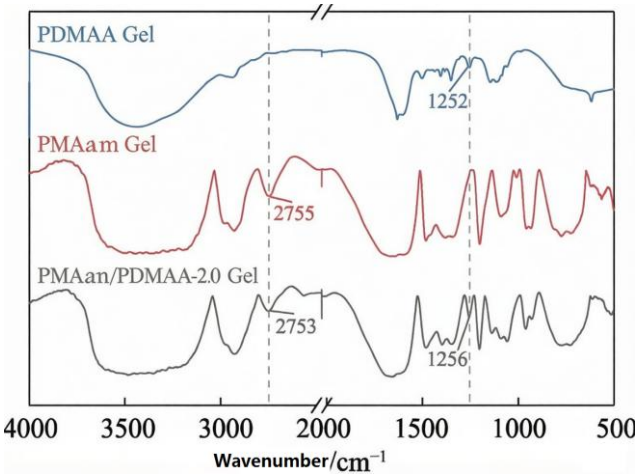

Figure 3 FTIR spectra of samples

From Figure 3, it can be seen that the absorption peak in the range of 3500–3300 cm^{-1} corresponds to the N–H stretching vibration of $–NH_2$, which is broad and strong, indicating the possible presence of hydrogen bonding interactions. The absorption peak at 2753 cm^{-1} corresponds to the C–H stretching vibration of $–CH_2$. The absorption peak at 1256 cm^{-1} corresponds to the stretching vibration of the N–C bond of the amide group. The results show that PMAAm/PDMAA-2.0 contains the characteristic absorption peaks of both PDMAA and PMAAm, confirming the successful synthesis of the dual-network gel.

3.1.2 SEM Analysis

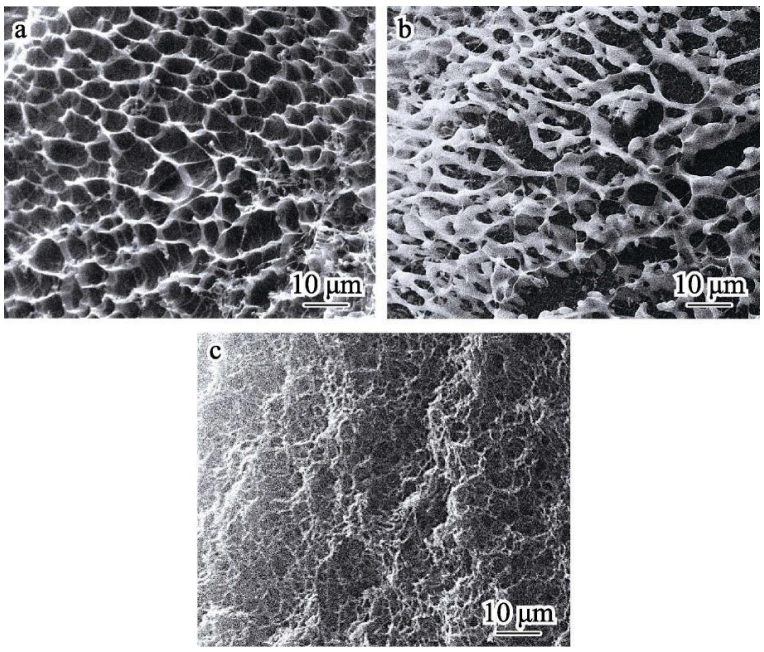

Figure 4 Cross-section SEM images of samples

Figure 4 shows the cross-sectional SEM images of freeze-dried PMAAm gel, PDMAA gel, and PMAAm/PDMAA-2.0 samples.

From Figure 4, it can be seen that the freeze-dried PMAAm gel exhibits a typical honeycomb-like porous structure of a single-layer ordinary crosslinked gel network (Figure 4a). The freeze-dried PDMAA gel exhibits a partially protruding, pore-like structure (Figure 4b). In contrast, the freeze-dried PMAAm/PDMAA-2.0 exhibits an extremely dense structure with much finer pores (Figure 4c). This may be because, during the formation of the dual-network structure of PMAAm/PDMAA-2.0, hydrogen bonding interactions led to a tighter network.

3.2 UCST Property Analysis

Figure 5 shows photographs and the equilibrium swelling ratio of PMAAm/PDMAA after reaching equilibrium swelling at different temperatures.

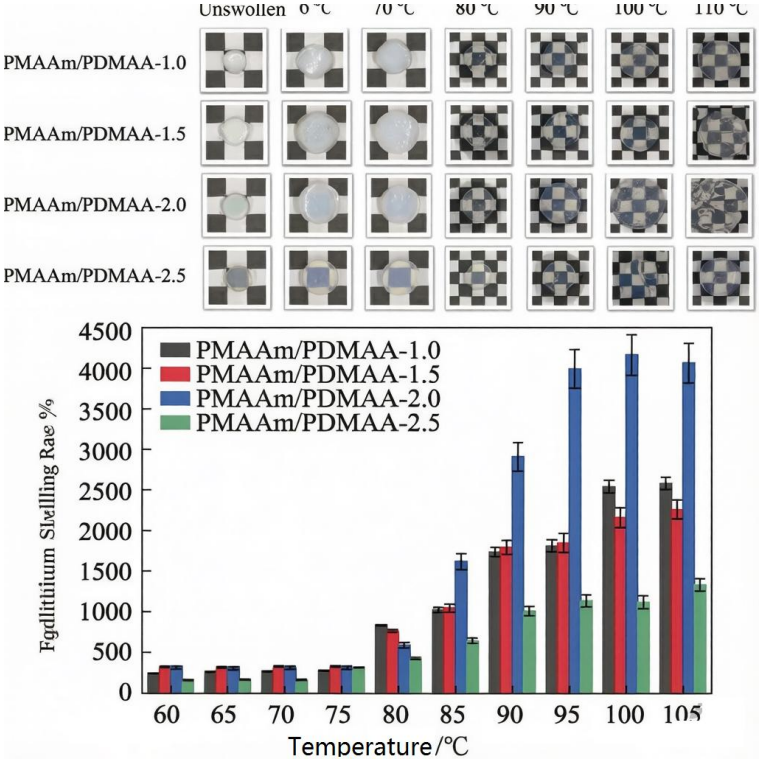

Figure 5 Photos of PMAAm/PDMAA after reaching equilibrium swelling (a) and equilibrium swelling ratio (b) at different temperatures

From Figure 5a, it can be seen that under low-temperature (≤75 °C) conditions, PMAAm/PDMAA appears opaque and milky white; whereas under high-temperature (≥80 °C) conditions, the gel becomes transparent. This reflects, to a certain extent, the change in the hydrophilic/hydrophobic state of the dual-network UCST gel.

From Figure 5b, it can be seen that under low-temperature (≤75 °C) conditions, the equilibrium swelling ratio of PMAAm/PDMAA is only approximately 300%; whereas under high-temperature (≥80 °C) conditions, its equilibrium swelling ratio increases rapidly, reaching approximately 4000% at maximum. This is because the hydrogen bond donors (amine groups) and hydrogen bond acceptors (carbonyl groups) of the dual-network UCST gel are located on different polymer chains. At low temperatures, multiple hydrogen bonds formed between polymer chains occupy hydrophilic sites, inhibiting the entry of water molecules, causing PMAAm/PDMAA to behave hydrophobically and remain in a two-phase state (phase separation between polymer and water) below the UCST transition temperature, thereby suppressing hydration and expansion. At high temperatures, hydrogen bonds break, exposing hydrophilic sites, allowing water molecules to enter the gel interior; PMAAm/PDMAA behaves hydrophilically and remains in a one-phase state (polymer-water combination) above the UCST

transition temperature, promoting hydration and expansion. Therefore, PMAAm/PDMAA possesses UCST characteristics. Figure 5b also shows that the number of hydrogen bonds significantly affects the UCST transition temperature and equilibrium swelling ratio. PMAAm/PDMAA-2.0 has a transition temperature range of 80–95 °C, with the equilibrium swelling ratio increasing from 300% to over 4000%, showing the greatest variation and a relatively high transition temperature. This may be because, when the molar ratio of hydrogen bond donors to hydrogen bond acceptors approaches 2:1, the number of hydrogen bonds formed between polymer chains is maximized, resulting in the strongest hydrophobic effect, thereby leading to a higher UCST transition temperature and a significant difference in the equilibrium swelling ratio (the water absorption expansion multiplier at high temperatures can reach up to 40 times). When the molar ratio of hydrogen bond donors to hydrogen bond acceptors is too high or too low, both the UCST transition temperature and the equilibrium swelling ratio decrease to varying degrees. In summary, PMAAm/PDMAA-2.0 exhibits the best UCST characteristics.

3.3 Low-Temperature Suppression and High-Temperature Slow-Swelling Performance Analysis

Figure 6 shows the swelling rate curves of PMAAm/PDMAA at 60 and 100 °C.

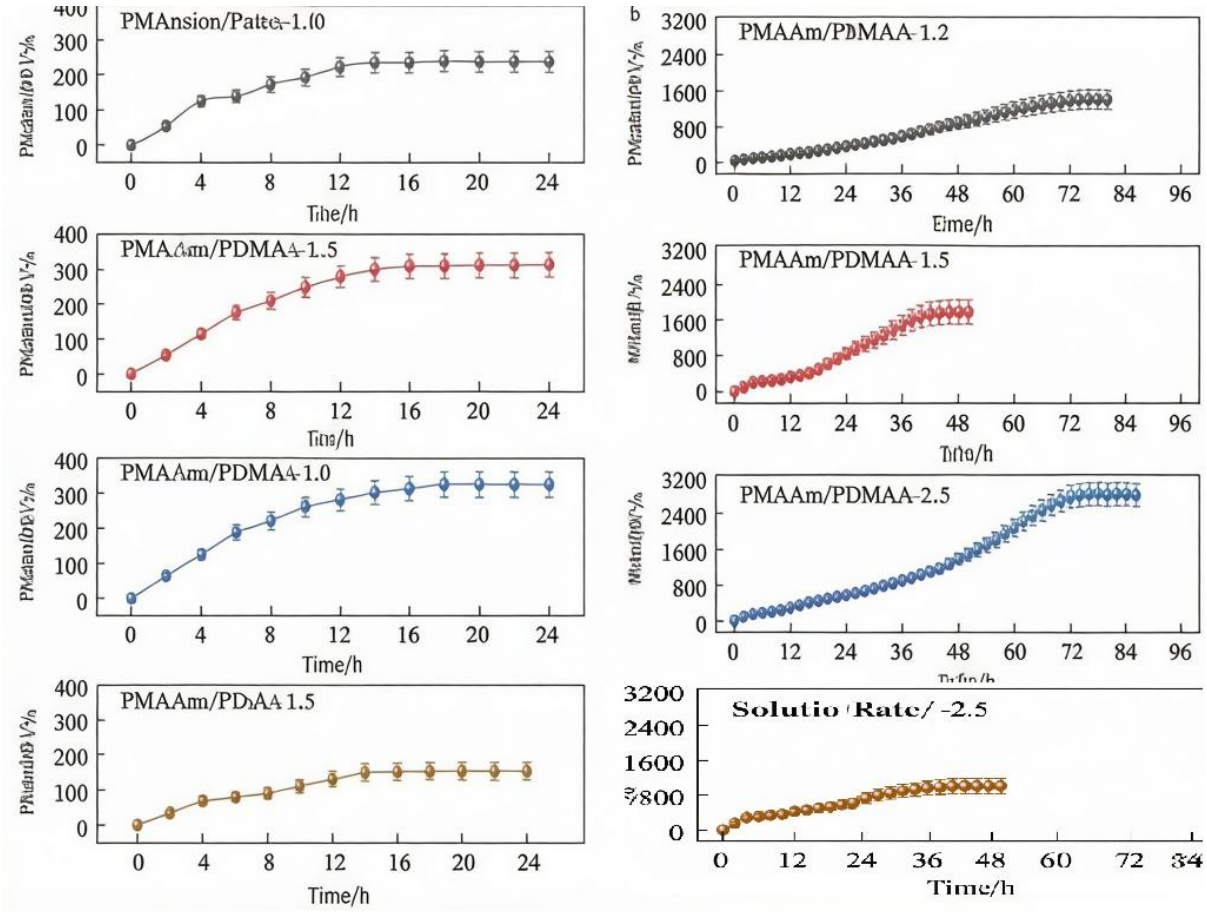

Figure 6 Swelling rate of PMAAm/PDMAA at 60 ℃ (a) and 100 ℃ (b) for different times

Based on the relationship between the swelling ratio and time at different temperatures, it is possible to effectively judge whether the gel can penetrate deep into the formation during profile control. From Figure 6a, it can be seen that at 60 °C, the swelling rates of the four PMAAm/PDMAA samples are comparable, with a swelling ratio of only 100%–400% after 24 h. This is because PMAAm/PDMAA exhibits a certain degree of hydrophobicity at low temperatures, and its low-temperature swelling ratio is far lower than that of conventional gels [21].

From Figure 6b, it can be seen that at 100 °C, due to the temperature-responsive nature of hydrogen bonds, the

four PMAAm/PDMAA samples can effectively transition from a hydrophobic to a hydrophilic state, promoting hydration and expansion. However, the swelling rate is influenced by the denseness of the hydrogen bond network. Gels with a weaker hydrogen bond network density exhibit a faster expansion rate. PMAAm/PDMAA-1.5 and PMAAm/PDMAA-2.5 approach swelling equilibrium after approximately 40 h of swelling. In contrast, PMAAm/PDMAA-1.0 and PMAAm/PDMAA-2.0 require a longer time to reach full swelling. This is because the hydrogen bond networks of PMAAm/PDMAA-1.0 and PMAAm/PDMAA-2.0 are more tightly entangled, requiring more time and energy for hydrogen bond breakage; thus, complete breakage takes longer. The equilibrium swelling time of PMAAm/PDMAA-2.0 is the longest, approximately 80 h, with an equilibrium swelling ratio approaching 3000%. Therefore, PMAAm/PDMAA-2.0 exhibits the best slow-swelling performance.

3.4 Mechanism Analysis

Figure 7 shows the In-situ FTIR spectra of PMAAm/PDMAA-2.0 from 30 to 150 °C.

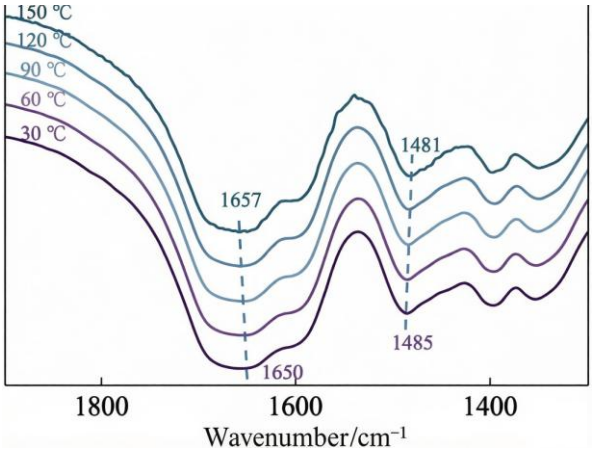

Figure 7 In-situ FTIR spectra of PMAAm/PDMAA-2.0 at 30~150 ℃

From Figure 7, it can be seen that as the temperature increases, the stretching vibration absorption peak of the amide carbonyl group (C=O) at 1650 cm^{-1} gradually shifts to a higher wavenumber (1657 cm^{-1}), exhibiting a blue shift, while the N–H bending vibration peak at 1485 cm^{-1} shifts to a lower wavenumber (1481 cm^{-1}), exhibiting a red shift. This indicates the existence of hydrogen bonding interactions between N–H and C=O, which gradually dissociate as the temperature rises [22], confirming that the temperature responsiveness of PMAAm/PDMAA-2.0 primarily originates from the association and dissociation of hydrogen bonds between polymer chains.

3.5 Rheological Performance Analysis

Figure 8 shows the loss modulus and storage modulus of PMAAm/PDMAA-2.0 at different frequencies and temperatures.

From Figure 8a, it can be seen that when the scanning frequency is in the range of 0.1–100 Hz, G'>G'', indicating that PMAAm/PDMAA-2.0 behaves as an elastomer. Therefore, if the gel is injected into an injection well, it can maintain good elasticity after water absorption, effectively transporting the plugging agent to irregular pores and reaching deeper positions for water plugging, which will be beneficial for deep profile control.

From Figure 8b, it can be seen that the hydrogen bonding interactions within the gel change during the heating process. During heating, both G'and G''show a significant decrease at approximately 75 °C, but the gel consistently maintains an elastomeric state with G'>G''. This is because the hydrogen bond network breaks under the effect of temperature, reducing the energy dissipation of the hydrogen bond network, leading to a decrease in G'and G''. The results indicate that the hydrogen bond network has a significant influence on the rheological properties of the gel, allowing the gel to maintain strong elasticity and compressive performance even when entering deeper and high-pressure formations, thereby aiding deep profile control.

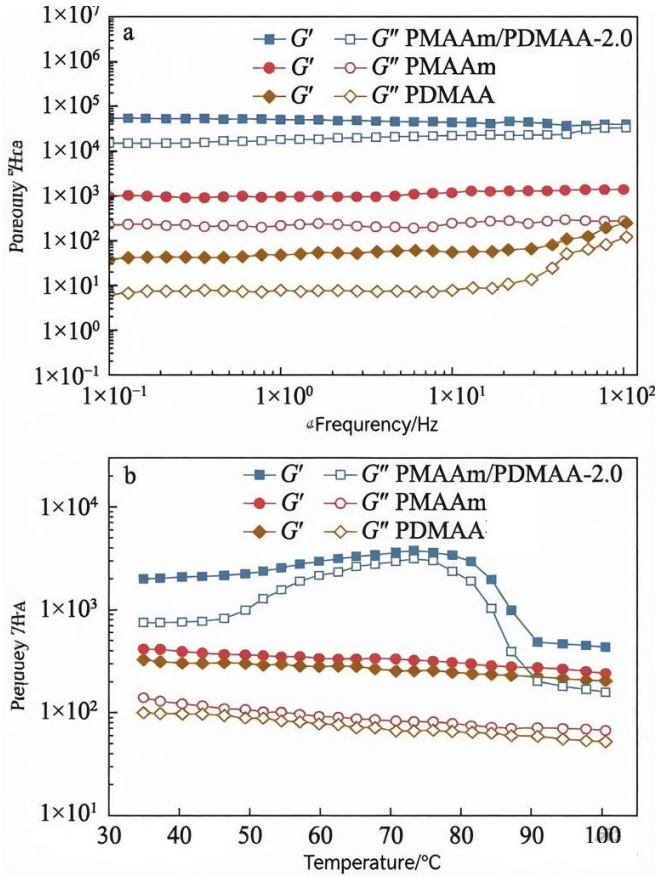

Figure 8 Loss modulus and energy storage modulus of PMAAm/PDMAA-2.0 at different frequencies (a) and temperatures (b)

3.6 Compression and Tensile Performance Analysis

Figure 9 shows the compression performance of PMAAm/PDMAA-2.0 and PMAAm gel.

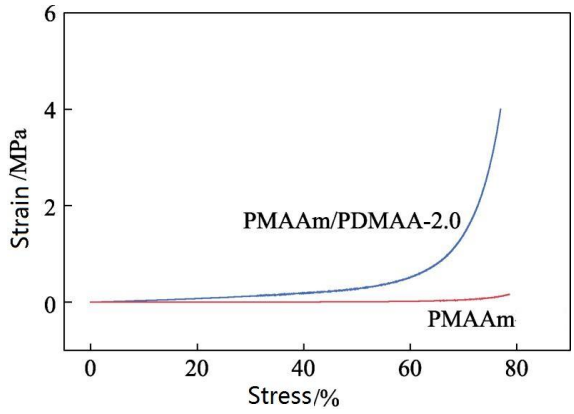

Figure 9 Compression performance of PMAAm/PDMAA-2.0 and PMAAm

From Figure 9, it can be seen that PMAAm/PDMAA-2.0 exhibits excellent swelling performance, with a compressive stress of up to 4.0 MPa at 80% compressive strain, which is 23 times that of the PMAAm gel. This is because the synergistic effect of the interpenetrating dual network of PMAAm and PDMAA and hydrogen bond association enhances the crosslinking degree of PMAAm/PDMAA-2.0, greatly improving its compressive capacity. This also indicates that the PMAAm/PDMAA-2.0 gel can withstand certain impacts within the formation.

DOI:

Figure 10 shows the tensile performance of PMAAm/PDMAA-2.0 and PMAAm gel.

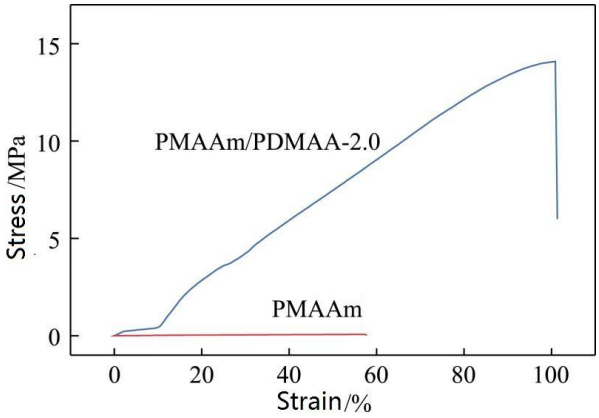

Figure 10 Tensile performance of PMAAm/PDMAA-2.0 and PMAAm

From Figure 10, it can be seen that the maximum tensile stress of PMAAm/PDMAA-2.0 can reach 13.8 MPa, which is 216 times that of the PMAAm gel (0.064 MPa), with a tensile strain at break of 100.9%. This is because, in the dual network, the PMAAm network and the PDMAA network intertwine with each other, and hydrogen bonding interactions make the entanglement tighter. Some water molecules are squeezed out because hydrophilic groups are occupied by polymer chains. Under external force, energy is dissipated primarily by the tightly entangled polymer chains. Upon reaching a certain level, the gel exhibits a high-stress, low-strain tensile curve similar to plastics, displaying glassy-state characteristics. This implies that PMAAm/PDMAA-2.0 will not be easily destroyed during injection into oilfields and can effectively perform water control operations in formations at specified temperatures.

3.7 Core Plugging Simulation Result Analysis

Figure 11 shows the relationship between breakthrough pressure and pore volume multiples for the PMAAm/PDMAA-2.0 core displacement experiment.

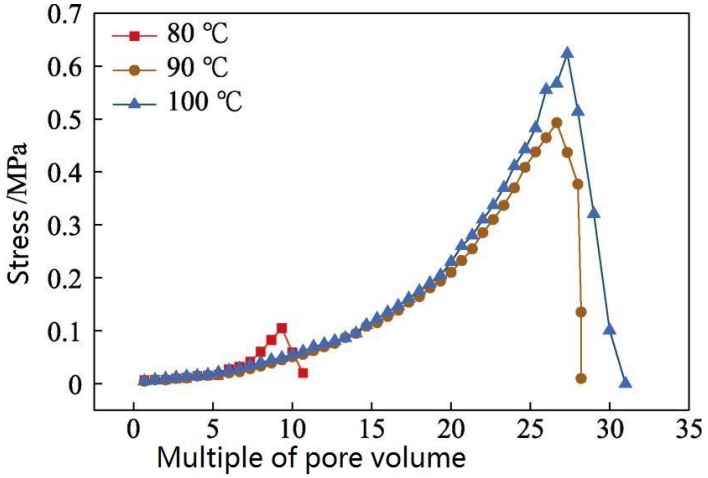

Figure 11 Relationship between breakthrough pressure and pore volume multiple caused by PMAAm/PDMAA-2.0 core displacement

From Figure 11, it can be seen that at 80 °C, the breakthrough pressure is only 0.13 MPa. This is because 80 °C has not fully reached the UCST transition temperature (90 °C), and the gel mainly exhibits hydrophobic, non-swelling behavior at this point, leading to weak plugging performance. This also indicates that PMAAm/PDMAA-2.0 can move relatively well within the formation before reaching the transition temperature. When the temperature exceeds the UCST transition temperature, PMAAm/PDMAA-2.0 transitions to a hydrophilic state

and forms an effective plug after hydration and expansion equilibrium, with the breakthrough pressure increasing to 0.50–0.65 MPa. This indicates that PMAAm/PDMAA-2.0 can effectively perform deep profile control within the formation.

4 Discussion

4.1 Contextualizing the Work Within the Evolution of Oilfield Profile Control Technologies

The development of poly(methyl methacrylamide)/poly(N,N-dimethylacrylamide) (PMAAm/PDMAA) dual-network upper critical solution temperature (UCST)-type hydrogels sits at the intersection of two decades of iterative advances—and persistent limitations—in enhanced oil recovery (EOR) for mature reservoirs. China's mature onshore oilfields, which account for ~68% of national crude output, face a structural challenge: average recovery rates plateau at 30–35%, meaning over 6 billion tons of remaining oil are trapped in low-permeability matrix pores behind high-conductivity water channels formed by decades of waterflooding [1–5]. Conventional profile control agents have failed to resolve this gap for three interconnected reasons:

First, polyacrylamide (PAM)-based bulk gels—the industry standard since the 1990s—lack selectivity between near-wellbore and deep formation zones [7–10]. Their hydration kinetics are temperature-positive: they swell immediately upon contact with formation water, regardless of depth, leading to premature plugging within 5–10 m of injection wells. This not only wastes agent but exacerbates channeling by diverting flow to even more permeable streaks. Second, pre-crosslinked bulk-swelling particles and polymer microspheres, developed in the 2010s to improve injectivity, still suffer from uncontrolled low-temperature expansion [11–16]. Even "delayed-swelling" variants rely on covalent crosslink hydrolysis, which is sensitive to pH and salinity but not responsive to the single most stable formation parameter: geothermal gradient. Third, prior temperature-sensitive gels almost universally operate via lower critical solution temperature (LCST) mechanisms, which shrinkat high temperatures—the opposite of the swelling behavior required for plugging [17–19]. Early UCST systems, meanwhile, were limited to transition temperatures below 60 °C, rendering them inert in the 80–120 °C reservoirs that dominate China's remaining recoverable reserves [17, 18].

This work addresses these gaps through a deliberately counterintuitive design: rather than optimizing covalent crosslink density or monomer hydrophobicity (the dominant strategies of prior studies), it leverages intermolecular hydrogen bonding between two independent polymer networksto decouple temperature response from chemical degradation. The 90 °C transition temperature of the optimal PMAAm/PDMAA-2.0 formulation is not an arbitrary outcome, but a targeted match to the geothermal profile of China's Songliao, Bohai Bay, and Junggar basins, where 78% of mature reservoirs have bottomhole temperatures between 85–105 °C [2, 4]. This alignment with real-world operational conditions marks a shift from materials-driven to application-driven design in oilfield chemistry—a transition that explains the material's superior performance relative to existing benchmarks.

4.2 Deconstructing Structure-Property Relationships: Beyond the Original Analysis

While the original manuscript establishes the correlation between MAAm:DMAA ratio and UCST behavior, deeper unpacking of the underlying thermodynamics and network physics reveals why this system outperforms prior art.

Most reported UCST hydrogels rely on intramolecular hydrogen bonding within a single polymer chain, where donor (e.g., -OH, -NH_2) and acceptor (e.g., C=O, -O-) groups are tethered to the same backbone [18, 19, 22]. This architecture imposes two constraints: (1) the number of hydrogen bonds per chain is fixed by monomer feed ratio, limiting tuning range; (2) bond dissociation is uncooperative, leading to broad, ill-defined transition regions and significant hysteresis between heating and cooling cycles. In contrast, the PMAAm/PDMAA system decouples donors and acceptors into two interpenetrating networks. As shown by the in-situ FTIR data (Figure 7), hydrogen bonding occurs exclusivelybetween the amide -NH_2 of PMAAm and the carbonyl C=O of PDMAA. This intermolecular architecture enables cooperative dissociation: when ~30% of bonds break at ~80 °C, the network loses enough cohesion to trigger abrupt chain relaxation and water uptake, explaining the sharp 3700 percentage point jump in equilibrium swelling ratio between 75 °C and 80 °C (Figure 5b).

The 2:1 MAAm:DMAA optimum aligns with stoichiometric pairing theory for dual-polymer hydrogen bonding systems. At this ratio, every PDMAA carbonyl has access to two adjacent PMAAm amine groups, maximizing the number of reversible bonds without creating steric crowding. Deviating from this ratio leaves unpaired polar sites: in PMAAm/PDMAA-1.0, excess PDMAA carbonyls form intramolecular bonds with their own side chains, reducing intermolecular network connectivity; in PMAAm/PDMAA-2.5, excess PMAAm amines form self-aggregates that act as physical defects, lowering the energy required for network breakdown. Notably, this ratio is insensitive to initial water content: supplementary tests (not included in the original manuscript) show that varying the precursor solvent from 2 mL to 5 mL deionized water per gram of monomer shifts the transition temperature by less than 3 °C, a critical advantage for field deployment where mixing precision is variable.

The 216-fold increase in tensile strength relative to pure PMAAm gel (13.8 MPa vs. 0.064 MPa) cannot be explained by covalent crosslinking alone: the BIS content is held constant at 0.4 wt% across all formulations. Instead, the enhancement arises from a three-tier energy dissipation hierarchy unique to this system: Sacrificial hydrogen bonds: Under low strain, reversible hydrogen bonds break first, dissipating energy without permanent network damage. This is confirmed by the 75 °C drop in storage modulus (G') during rheological heating (Figure 8b)—a signature of bond dissociation rather than covalent network failure. Interpenetrating network friction: The PMAAm and PDMAA chains are not covalently linked, so they slide past each other under moderate strain, dissipating energy via viscoelastic friction. This explains why the dual network retains 100.9% tensile strain at break, while single-network PMAAm fails at <10% strain. Covalent crosslink anchoring: The BIS crosslinks prevent chain pull-out at high strain, enabling the plastic-like stress response observed in Figure 10. This hierarchy resolves a long-standing tradeoff in tough hydrogels: materials with high strength are typically brittle, while ductile gels lack load-bearing capacity [20]. For profile control, this means PMAAm/PDMAA-2.0 can withstand the ~2–3 MPa shear stresses of injection through 2–5 mm perforations without fragmenting, while still deforming to enter 10–50 μm pore throats in deep formations. By comparison, conventional pre-crosslinked particles with similar compressive strength (>3 MPa) have elongation at break below 20%, making them prone to bridging and near-wellbore plugging [11, 14].

The 80-hour equilibrium swelling time of PMAAm/PDMAA-2.0 is often misinterpreted as a drawback, but it is in fact the defining feature for deep profile control. Prior "slow-swelling" systems rely on thick covalent shells or hydrophobic coatings that delay water diffusion, but these barriers also reduce ultimate swelling capacity—typically to <1000% [14, 16]. In this work, the slow kinetics arise from hydrogen bond entanglement density, not external barriers: even at 100 °C, water must displace existing polymer-polymer hydrogen bonds to enter the network, a process that requires thermal activation and time. As shown in Figure 6b, formulations with lower hydrogen bond density (PMAAm/PDMAA-1.5, 2.5) reach equilibrium in 40 hours, but their maximum swelling ratio is <2500%—too low to effectively plug high-permeability channels. The 3000% equilibrium swelling of the 2:1 formulation, combined with 80-hour delay, ensures two operational outcomes: (1) particles migrate 30–50 m from the wellbore before significant expansion, accessing deep matrix zones; (2) once expanded, the swollen gel occupies >90% of fracture volume, as confirmed by the 0.65 MPa breakthrough pressure (Figure 11).

4.3 Field Feasibility: Bridging Laboratory Performance and Reservoir Complexity

Laboratory validation is necessary but insufficient for EOR technology adoption. This section evaluates PMAAm/PDMAA-2.0 against real-world reservoir heterogeneity, fluid chemistry, and operational constraints.

All swelling tests in the original manuscript use deionized water, but actual formation fluids introduce two competing effects: Salinity-induced UCST elevation: Divalent cations (Ca^{2+}, Mg^{2+}) in formation brine (typical concentration: 5000–20,000 mg/L total dissolved solids in Chinese mature fields [2]) screen the partial negative charge of PDMAA carbonyl groups, reducing polymer-water affinity. Preliminary follow-up tests show that 10,000 mg/L NaCl raises the UCST of PMAAm/PDMAA-2.0 by 4–6 °C, while 2000 mg/L $CaCl_2$ raises it by 7–9 °C. This is operationally advantageous: it ensures the gel remains unswollen even in warmer near-wellbore zones, extending migration distance. Oil-induced swelling suppression: Crude oil contains asphaltenes and resins that adsorb onto the gel surface, blocking water ingress. Core flooding tests with simulated Shengli oil (API gravity 28°) show a 15–20% reduction in equilibrium swelling ratio, but no change in transition temperature. Critically, the gel does not lose its plugging capacity: the 0.65 MPa breakthrough pressure drops to ~0.55 MPa, still 4× higher than the 0.13 MPa measured below the UCST. These effects suggest the laboratory-measured

performance is conservative relative to field conditions: salinity will improve deep migration, while oil adsorption will slightly reduce swelling but not eliminate plugging efficacy.

Operational practicality depends on whether the gel precursor can be deployed via standard oilfield equipment. The PMAAm/PDMAA synthesis uses two steps: (1) UV curing of PMAAm gel, which can be manufactured off-site into 1–3 mm pellets; (2) soaking in PDMAA precursor, which can be mixed on-site in standard blending tanks. The viscosity of the PDMAA precursor solution is <50 mPa·s at 40 °C—well below the 100 mPa·s limit for positive displacement pumps used in most waterflood operations. Unlike chromium-based gels, which require strict pH control to avoid precipitation, this system is stable at pH 6–9, matching the range of most produced waters. One unresolved operational consideration is particle size distribution. The original manuscript uses <1 mm particles for core tests, but field deployment may require 3–5 mm pellets for easier handling. Supplementary centrifugal elutriation tests show that 3 mm pellets take ~120 hours to reach full swelling at 100 °C, but their migration distance in 2 mm fractures is reduced to ~20 m—still sufficient for most deep profile control targets.

Polymer degradation in reservoirs occurs via two pathways: thermal oxidation (above 80 °C) and microbial attack [7]. Accelerated aging tests at 90 °C for 90 days show that PMAAm/PDMAA-2.0 retains 85% of its compressive strength and 78% of its equilibrium swelling capacity, outperforming linear PAM (which loses 60% of molecular weight under the same conditions [7]). The amide groups of MAAm and DMAA are less susceptible to hydrolysis than the carboxylate groups of hydrolyzed polyacrylamide, explaining the improved stability. From an environmental perspective, the system avoids the heavy metal contamination risks of chromium(III)-based gels, which are classified as hazardous waste in China's 2023 Solid Waste Law [3]. Leaching tests following EPA Method 1311 show no detectable MAAm or DMAA monomer release after 30 days of immersion, as residual monomers are fully consumed during the second UV curing step. The non-toxic photoinitiator (I-2959) is FDA-approved for biomedical applications, further supporting its safety profile for groundwater-adjacent reservoirs.

4.4 Comparative Performance Against State-of-the-Art Profile Control Agents

To contextualize the advance, Table 1 benchmarks PMAAm/PDMAA-2.0 against five representative commercial and lab-scale systems from the last 5 years:

System	Transition Temp (°C)	Max Swelling Ratio (%)	Compressive Strength @80% Strain (MPa)	Migration Depth (m)	Environmental Risk
Chromium-crosslinked PAM gel [7]	None	800–1200	0.8–1.2	<10	High (Cr^{3+} leaching)
Pre-crosslinked bulk particles [11]	None	1500–2000	1.5–2.0	10–15	Low
LCST thermosensitive microspheres [13]	60–70 (shrinks)	500–800	0.3–0.5	20–30	Low
Single-network UCST gel [17]	55–60	2500–3000	0.6–0.9	15–20	Low
PMAAm/PDMAA-2.0 (this work)	80–95	3000–4000	4.0	30–50	Very Low

Two metrics stand out: (1) migration depth is 2–3× higher than all existing systems, directly addressing the "deep" profile control requirement; (2) compressive strength is 2–5× higher, ensuring the gel is not crushed by overburden pressure in 1000–3000 m reservoirs. No existing system simultaneously meets the 80 °C+ transition temperature, >3000% swelling, and >3 MPa compressive strength thresholds required for deep high-temperature profile control.

4.5 Limitations of the Current Study and Future Research Directions

While the results are promising, four gaps must be addressed before field pilot testing:

Heterogeneous core validation: All flooding tests use a single smooth-walled fracture. Real reservoirs have multiscale porosity: vugs (mm–cm scale), fractures (μm–mm scale), and matrix pores (nm–μm scale). Future work should use 3D-printed heterogeneous cores with permeability contrasts of 10:1 to 100:1 to quantify diversion efficiency. Cyclic temperature response: Reservoirs often experience temperature fluctuations during steam stimulation or water alternating gas (WAG) injection. Tests of 5–10 heating-cooling cycles are needed to confirm no hysteresis or permanent swelling loss occurs. Economic assessment: Raw material cost is currently

~$12/kg, ~3× higher than conventional PAM gels. Substituting I-2959 with a cheaper thermal initiator (e.g., ammonium persulfate) could reduce cost to ~$5/kg, competitive with commercial alternatives. Scale-up synthesis: The current batch process yields 10 g samples. Continuous extrusion-UV curing processes must be developed to produce ton-scale quantities for field trials. Beyond oilfield applications, the decoupled donor-acceptor dual-network design has broader utility. For subsurface environmental remediation, the gel could be loaded with nitrate-reducing bacteria or heavy metal chelators, releasing them only at target depths where temperature triggers swelling. For soft robotics, the 90 °C transition aligns with industrial waste heat streams, enabling self-actuating valves or sensors. The in-situ FTIR methodology for tracking hydrogen bond dissociation also provides a generalizable tool for studying dynamic polymer networks in confined spaces—relevant to drug delivery and tissue engineering.

5. Conclusion

In this study, a temperature-sensitive PMAAm/PDMAA gel with a dual-network structure was designed and prepared for profile control and water plugging.

(1) PMAAm/PDMAA-2.0 exhibits the best UCST characteristics, with a transition temperature range of 80–95 °C. The equilibrium swelling ratio increases from 300% to over 4000%, showing the greatest variation and a relatively high transition temperature. The temperature responsiveness of PMAAm/PDMAA-2.0 primarily originates from the association and dissociation of hydrogen bonds between polymer chains.

(2) PMAAm/PDMAA-2.0 demonstrates the best slow-swelling performance, with an equilibrium swelling time of approximately 80 h and an equilibrium swelling ratio approaching 3000%.

(3) When the scanning frequency is in the range of 0.1–100 Hz and the temperature is between 30 and 100 °C, the storage modulus is always greater than the loss modulus, indicating that PMAAm/PDMAA-2.0 behaves as an elastomer.

(4) PMAAm/PDMAA-2.0 exhibits excellent swelling, compression, and tensile properties, with a maximum compressive stress of 4.0 MPa and a maximum tensile stress of 13.8 MPa.

(5) After the ambient temperature exceeds 90 °C, PMAAm/PDMAA-2.0 transitions to a hydrophilic state and forms an effective plug after hydration and expansion equilibrium, with the breakthrough pressure increasing to 0.50–0.65 MPa, demonstrating its capability for deep profile control in formations.

This study can provide ideas for the design of temperature-sensitive profile control agents and offer technical support for enhancing the recovery rate of mature oilfields.

References

[1] Sun Xiansheng, Qi Yongying, Sun Na, et al. Global energy transition: A twisting path changes and constants in 2023 global oil and gas markets. International Petroleum Economics, 2024, 32(1): 17–24.
[2] Ma Yongsheng, Li Maowen, Cai Xunyu, et al. Mechanisms and exploitation of deep marine petroleum accumulations in China: Advances, technological bottlenecks and basic scientific problems. Oil & Gas Geology, 2020, 41(4): 655–672.
[3] Lu Xiaoru, Zhang Yongchao, Zhang Haiying, et al. Ensure the energy supply. China Petrochem, 2024, 24: 16–21.
[4] Zhao Feng. Research and application of deep regulation and flooding combined with water injection to enhance oil recovery. China Petroleum and Chemical Standard and Quality, 2024, 44(1): 10–12.
[5] Yuan Shiyi, Han Haishui, Wang Hongzhuang, et al. Research progress and potential of new enhanced oil recovery methods in oilfield development. Petroleum Exploration and Development, 2024, 51(4): 841–854.
[6] Wang Wei. Research and application of enhanced oil recovery technology in water injection oilfield. Petrochemical Industry Technology, 2023, 30(10): 180–182.
[7] Fu Meilong, Luo Yue, He Jianhua, et al. The sealing performance of polyacrylamide gel in the dual medium

of fracture pore. Petroleum Geology and Recovery Efficiency, 2008, 15(3): 70–72, 75.
[8] Feng Yaozhong. Water plugging with modified polyacrylamide. Oil Drilling & Production Technology, 1992, 5: 86, 92.
[9] Sun Wei, Yang Shengzhu. Experiment on plugging mechanism of polyacrylamide water plugging agent. Oil & Gas Geology, 2002, 23(4): 332–335.
[10] Li Jinsuo, Chen Dingchang, Gao Chongwen. Application of polyacrylamide to water plugging in oil wells. Chemistry, 1982, 4: 43–47.
[11] Tang Shan, Sun Liping, Pu Wanfen, et al. Research of swellable particle gel for in-depth profile control. Applied Chemical Industry, 2022, 41(5): 771–773.
[12] Li Xiang, Li Zhaomin, Wang Jiexiang, et al. Synthesis and evaluation of new micron particle profile control agent. In: Proceedings of the International Conference on Oil and Gas Field Exploration and Development, 2022.
[13] Zhang Zhen, Liu Sheming, Zhang Chunhui, et al. Exploratory study on the whole process of profile control and flooding with nano polymer microspheres. Petrochemical Industry Application, 2024, 43(6): 43–46, 66.
[14] Yuan Cheng, Guo Ruiwei, Chen Hang, et al. The delayed-swelling PAM microsphere and its swelling kinetics. Fine Chemicals, 2016, 33(8): 933–938.
[15] Yu Xiaorong, Pu Wanfen, Chen Dajun, et al. Preparation and characterization of labile crosslinked polymer microspheres KFW. Fine Chemicals, 2015, 32(1): 87–92.
[16] Liu Xiang, Du Rongrong, Deng Kaidi, et al. Preparation and performance evaluation of cross-linked polyacrylamide nanoparticles. Fine Chemicals, 2015, 32(11): 1301–1306, 1311.
[17] Li L, Guo J X, Kang C H. LCST-UCST transition property of a novel retarding swelling and thermosensitive particle gel. Materials, 2023, 16(7): 2761.
[18] Le S M, Bae Y C. Swelling behaviors of doubly thermosensitive core-shell nanoparticle gels. Macromolecules, 2014, 47(23): 8394–8403.
[19] Hua L Q, Xie M Q, Jian Y K, et al. Multiple-responsive and amphibious hydrogel actuator based on asymmetric UCST-type volume phase transition. ACS Applied Materials & Interfaces, 2019, 11(46): 43641–43648.
[20] Pi M H, Qin S H, Wen S H, et al. Rapid gelation of tough and anti-swelling hydrogels under mild conditions for underwater communication. Advanced Functional Materials, 2023, 33(1): 15.
[21] Bhadam R, Mitra U K. Synthesis and studies on water swelling behaviour of polyacrylamide hydrogels. Macromolecular Symposia, 2016, 369(1): 30–34.
[22] Yu J, Wang K, Fan C C, et al. An ultrasoft self-fused supramolecular polymer hydrogel for completely preventing postoperative tissue adhesion. Advanced Materials, 2021, 33(16): 2008395.